Determination of the Spin Polarization of Half-Metallic CrO_2 by Point Contact Andreev Reflection

Y. Ji,[1] G. J. Strijkers,[1] F. Y. Yang,[1] C. L. Chien,[1] J. M. Byers,[2] A. Anguelouch,[3] Gang Xiao,[3] and A. Gupta[4]
[1]*Department of Physics and Astronomy, The Johns Hopkins University, Baltimore, Maryland 21218*
[2]*Naval Research Laboratory, Washington, D.C. 20375*
[3]*Department of Physics, Brown University, Providence, Rhode Island 02912*
[4]*IBM T. J. Watson Research Center, Yorktown Heights, New York 10598*
(Received 15 November 2000)

Andreev reflection at a Pb/CrO_2 point contact has been used to determine the spin polarization of single-crystal CrO_2 films made by chemical vapor deposition. The spin polarization is found to be 0.96 ± 0.01, which confirms that CrO_2 is a half-metallic ferromagnet, as theoretically predicted.

DOI: 10.1103/PhysRevLett.86.5585 PACS numbers: 74.80.Fp, 75.30.–m, 75.70.–i

Traditional electronic devices are based on the manipulation of electrical charge. In recent years, magnetoelectronic devices, such as spin-valve field sensors and magnetic random access memories, have emerged, where both charge and spin of electrons are exploited using spin-polarized currents and spin-dependent conduction [1,2]. The performance of such magnetoelectronic devices depends critically on the substantial spin polarization P of the ferromagnetic components.

Of particular interest are the so-called half-metallic ferromagnets [3], which are completely spin polarized with $P = 1$. In a magnetic tunnel junction with half-metallic electrodes, one would have the exciting prospect of switching between conducting and insulating states when the relative orientations of the magnetization vectors of the two electrodes are altered [4]. Chromium dioxide (CrO_2) is a ferromagnetic oxide that is theoretically predicted to be half metallic [5–7]. This, combined with its favorable switching behavior at small fields [8], makes CrO_2 a strong candidate for low-field magnetoresistance devices. It is therefore essential to accurately determine the spin polarization of CrO_2 experimentally.

Recently, it was shown that point-contact Andreev reflection (PCAR) can be used to determine the spin polarization of a metal [9–11]. The method uses the fact that the Andreev reflection probability at a superconductor/metal interface is limited by the carrier density of the minority spin band at the Fermi level in the metal. In the limit of a clean ballistic superconductor/metal contact without interfacial scattering, the spin polarization P of the conduction electrons [12] can be determined from $G(0)/G_n = 2(1 - P)$, with $G(0)$ and G_n the conductance at zero and high bias voltage, respectively. Previously, the spin polarization of polycrystalline CrO_2 was determined using this PCAR technique [11,13]. However, for the conductance behavior of real contacts, which are seldom in the clean limit, $G(0)/G_n = 2(1 - P)$ cannot be assumed, because this results in an exaggerated P value [14]. Furthermore, because of the metastable nature of CrO_2, most properties, including the spin polarization, depend critically on the quality of the CrO_2 material.

In this Letter, we report on an accurate determination of the spin polarization of *single-crystal* CrO_2 films. We show that it is necessary to analyze the complete conductance-voltage curve using a modified Blonder-Tinkham-Klapwijk (BTK) model [15] to extract the polarization reliably. This method will be illustrated by PCAR measurements of Ni, and subsequently applied to the single-crystal CrO_2. Most importantly, we demonstrate experimentally that CrO_2 with $P_{CrO_2} = 0.96 \pm 0.01$ is indeed a half-metallic ferromagnet.

Single-crystal chromium dioxide films have been grown on (100)-oriented single crystal TiO_2 substrates by chemical vapor deposition (CVD) using CrO_3 as a precursor [16]. The thickness of the films studied in this work is about 2000 Å. Figure 1(a) shows a typical θ-2θ x-ray diffraction pattern, which shows only the (200) and (400) peaks of CrO_2 and TiO_2. The rocking curve of the CrO_2 (200) peak is shown in Fig. 1(b), which has a full width at half maximum of only 0.11°, confirming the high structural quality of the film. The x-ray pole figures confirm that the CrO_2 film is a single crystal in epitaxial registry with the TiO_2 substrate [8].

PCAR measurements were performed using Nb tips for Ni and Pb tips for CrO_2. The tips were prepared by mechanical polishing from 0.030 in. diameter wires followed by electrochemical etching. The PCAR measurements were administered by a differential screw mechanism so that the tip can be microscopically moved towards the film surface [17]. The measuring setup was enclosed in a vacuum jacket and immersed in a liquid helium bath. Conventional four-probe measurements were employed to measure the conductance-voltage characteristics at 4.2 K for Ni and 1.85 K for CrO_2. A lock-in amplifier was used to measure the conductance by an ac-modulation method at a frequency of 2007 Hz. By varying the contact area mechanically, many PCAR measurements with different contact resistances were performed on the same film using

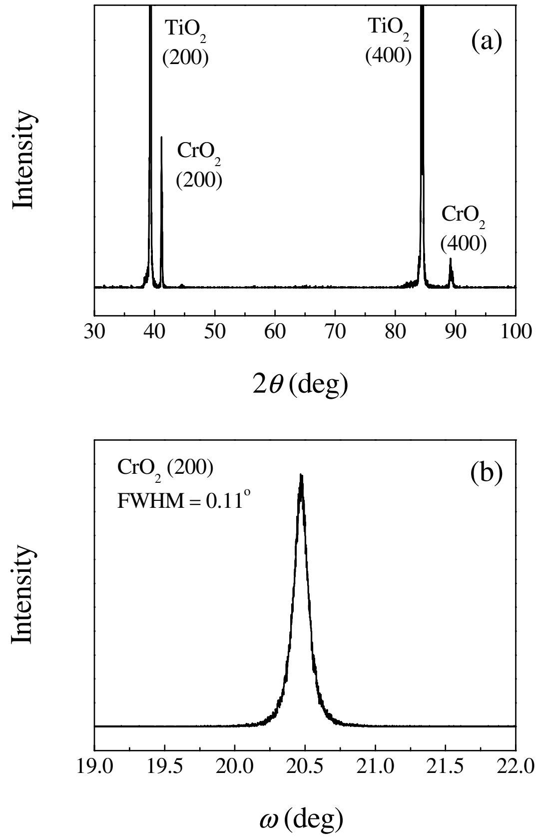

FIG. 1. (a) θ-2θ x-ray diffraction pattern of the CrO_2 film on a TiO_2 (100) substrate, which shows only the (200) and (400) peaks of CrO_2 and TiO_2. (b) The rocking curve of CrO_2 peak has a full width at half maximum (FWHM) of 0.11°.

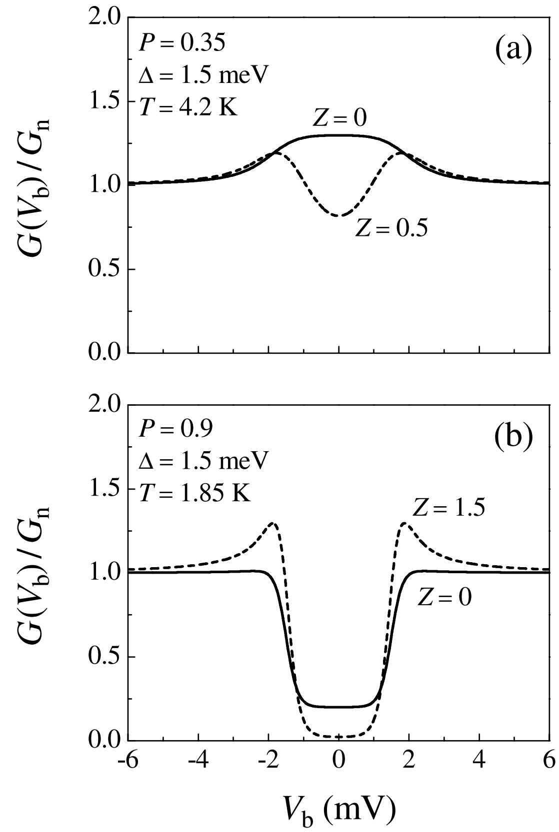

FIG. 2. Calculated normalized conductance $G(V_b)/G_n$ versus bias voltage V_b using the modified BTK model for (a) $P = 0.35$, $T = 4.2$ K and (b) $P = 0.9$, $T = 1.85$ K. The solid lines are for $Z = 0$, and the dashed lines are for $Z > 0$.

the same tip. This is a distinct advantage of the PCAR measurements using a mechanical tip. In contrast, other measurements of P using tunnel junctions [18] or nanolithography structures [10] are contingent upon the fabrication, and, furthermore, the characteristics of the interface are unique to each structure and cannot be altered.

To analyze the experimental conductance-voltage curves and extract P we use a modified version of the BTK model [15]. The spin polarization P of the metal was included by dividing the polarized current into two parts: a completely unpolarized part, for which Andreev reflections are allowed, and a fully polarized part, for which the Andreev reflection probability is zero. Interfacial scattering is modeled via a δ-function potential at the interface with a dimensionless height Z. More details about this model and the calculations can be found in Ref. [14]. As an example Figs. 2(a) and 2(b) show calculated conductance-voltage curves for $P = 0.35$ and $P = 0.9$, respectively. When $Z = 0$ (solid lines), the curves show a characteristic bell shape for which $G(V_b)/G_n = 2(1 - P)$ for a bias voltage $|V_b| < \Delta$ and $G(V_b)/G_n = 1$ for $|V_b| \gg \Delta$, where 2Δ is the superconducting gap. However, for a nonideal contact with an interfacial scattering barrier, represented by a nonzero Z (dashed lines), $G(V_b)/G_n$ deviates considerably from that of a clean contact. Peaks develop at $-\Delta$ and Δ, and the conductance at zero bias voltage $G(0)/G_n$ drops sharply. This decrease of the zero-bias conductance can easily be mistaken for a larger spin polarization. From this we can conclude that the spin polarization P cannot be extracted reliably from the zero-bias conductance, but an analysis is needed of the complete experimental conductance-voltage curve.

To illustrate this method, Figs. 3(a)–3(d) show a representative selection of PCAR measurements (open circles) at $T = 4.2$ K for Nb on Ni for four different contact resistances R. Except for the conductance-voltage curve in Fig. 3(d), which displays the bell-shaped curve of a clean contact without interfacial scattering, the shape of the other curves is characteristic for a contact with a barrier that can be represented by a nonzero Z, similar to the theoretical curves shown in Fig. 2(a). All the curves can be fitted very well by the modified BTK model as illustrated by the solid lines in the figure using three parameters: spin polarization P_f, superconducting gap value Δ, and interfacial scattering barrier strength Z. The values of P_f, Δ, and Z resulting from the fits are shown in the figure.

Figure 3(e) shows that there is a systematic variation of the fitted spin polarization P_f with the barrier strength Z.

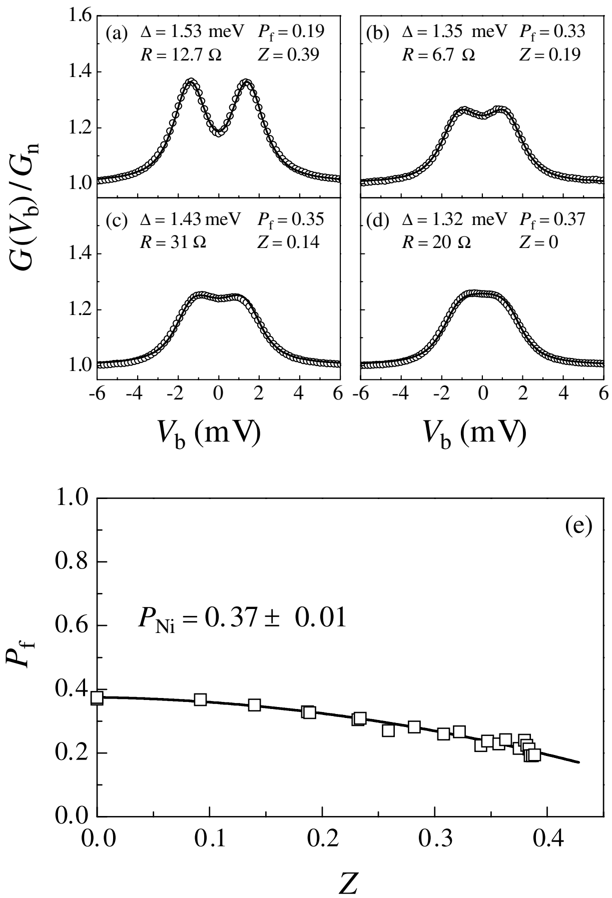

FIG. 3. (a)–(d) Measured $G(V_b)/G_n$ versus V_b of Nb/Ni point contacts at $T = 4.2$ K for different contact resistances (open circles). The solid lines are fits to the data with the BTK model resulting in P_f, Z, and Δ as indicated in the figure. (e) Fitted polarization P_f as a function of Z. The solid line is a polynomial fit of the data to extract the spin polarization $P_{Ni} = 0.37 \pm 0.01$ in the limit of $Z = 0$.

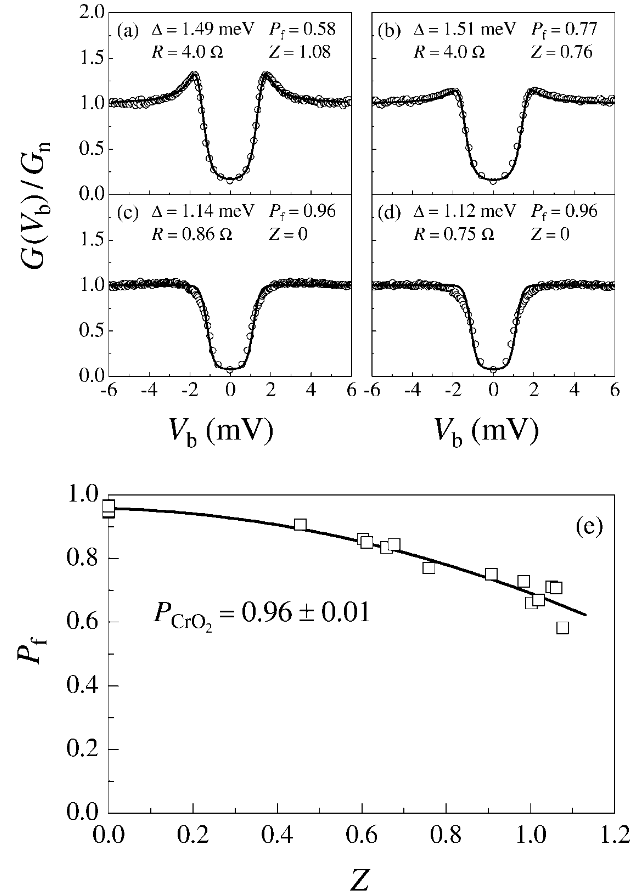

FIG. 4. (a)–(d) Measured $G(V_b)/G_n$ versus V_b of Pb/CrO_2 point contacts at $T = 1.85$ K for different contact resistances (open circles). The solid lines are fits to the data with the BTK model resulting in P_f, Z, and Δ as indicated in the figure. (e) Fitted polarization P_f as a function of Z. The solid line is a polynomial fit of the data to extract the spin polarization $P_{CrO_2} = 0.96 \pm 0.01$ in the limit of $Z = 0$.

In general, an increase of Z leads to a decrease of the spin polarization. This is due to negative effects of a scattering barrier on the spin polarization. Formation of NiO and Ni/Nb alloying cause spin-mixing effects and dilute the intrinsic spin polarization of the bulk. The bulk spin polarization of Ni can be extracted in the limit of $Z = 0$, resulting in $P_{Ni} = 0.37 \pm 0.01$. This value of the spin polarization for Ni is higher than $P_{Ni} = 0.29$ recently obtained by Monsma *et al.* [19], using a superconducting tunnel junction. However, Ni-alumina alloy formation is a problem in these tunnel junctions which considerably reduces the apparent spin polarization of Ni obtained by this method [20].

Representative measurements (open circles) of $G(V_b)/G_n$ versus V_b for Pb/CrO_2 at $T = 1.85$ K are shown in Figs. 4(a)–4(d). The contact resistances range between approximately 0.75 and 5.0 Ω, which corresponds to contact diameters between approximately 200 and 800 Å. We estimate from the electrical resistance that the carrier mean free path in CrO_2 is of the order of a 1000 Å, which indicates that the electrical transport is ballistic. We note, however, that for a correct determination of the spin polarization using our modified BTK model, ballistic transport is not a stringent requirement. Diffusive scattering merely leads to an increase in the fitted value of Z [21]. Nevertheless, the fact that we obtain some point contacts with $Z = 0$ is a strong indication that the transport is indeed ballistic.

In Figs. 4(a) and 4(b), there is a prominent peak at the gap values of the superconductor due to strong interfacial scattering, similar to the calculated curves in Fig. 2(b). In Figs. 4(c) and 4(d), however, these peaks are absent and the conductance is almost perfectly flat for $|V_b| > \Delta$, which means that the Pb/CrO_2 interface is clean with negligible interfacial scattering. The experimental data of the differential conductance has been analyzed using the modified BTK theory, similar to the Nb/Ni data shown before. All the experimental conductance curves can be fitted well, as illustrated by the solid lines in Figs. 4(a)–4(d). The fitted values of P_f, Z, and Δ are shown in the figure. The importance of the analysis of the full conductance curve of CrO_2 should be emphasized. The value of $P_{CrO_2} = 0.92$ would be concluded from Fig. 4(a), as reported in Ref. [11], based on the normalized conductance at zero bias voltage $G(0)/G_n$, while the actual P_f value is only 0.58. In Figs. 4(c) and 4(d) there is a discrepancy between the fitted and measured curves for bias voltages around the superconducting gap values. Moreover, the fitted gap value is lower than for the point contacts with $Z \neq 0$. We think that some induced superconductivity in the CrO_2 (proximity effect) leads to a suppression of the superconductivity and a distribution of gap values. The proximity effect can be incorporated into the model by introducing two or more gap values [14]. However, this has almost no influence on the fitted magnitude of the spin polarization of CrO_2.

Similar to Ni, the fitted spin polarization P_f for CrO_2 displays a systematic decrease with increasing barrier strength Z, as shown in Fig. 4(e). Most importantly, the spin polarization $P_{CrO_2} = 0.96 \pm 0.01$ can be uniquely defined from P_f in the limit of $Z = 0$. Indeed, CrO_2 is close to half metallic as widely believed. X-ray photoemission spectroscopy measurements of the film indicate the presence of a degraded surface layer with Cr_2O_3 and other unidentified chromium compounds (possibly chromium hydroxides), which may be responsible for the rapid decrease of the polarization at higher Z. In order to obtain a clean contact with $Z = 0$, we have to pierce this surface barrier layer with the Pb tip. It is not guaranteed that we have succeeded in completely removing all of this surface material even in the limit of $Z = 0$, and in this respect $P_{CrO_2} = 0.96 \pm 0.01$ represents a lower limit to the polarization.

Obviously, half-metallic CrO_2 is a very promising material for application in magnetic tunnel junctions. Its high spin polarization promises a tunnel magnetoresistance much larger than observed so far in CoFe based tunnel junctions [22]. The CVD deposition method allows for preparation on TiO_2 and Al_2O_3, which both may be suitable tunnel-barrier materials [23,24]. However, since electron tunneling occurs mainly from a few interfacial layers close to the tunnel barrier [25], a surface layer of degraded CrO_2, as observed in this study, will be undesirable. We have observed that with time (in the period of over a few weeks) it becomes harder and finally impossible to realize a clean point contact with $Z = 0$ in the PCAR measurements, using a bare CrO_2 film, which means that the surface degradation becomes worse over time. This problem may be circumvented by fabrication of tunnel junctions using multichannel CVD.

In conclusion, we have used Andreev reflection at a Pb/CrO_2 point contact to determine the spin polarization of single-crystal CrO_2 made by chemical vapor deposition. The spin polarization is found to be 0.96 ± 0.01, which confirms that, as theoretically predicted, CrO_2 is close to a half-metallic ferromagnet. A surface barrier layer strongly reduces the apparent spin polarization of CrO_2, which may have important consequences for a successful application of CrO_2 in magnetic tunnel junctions.

This work was supported by NSF Grants No. DMR96-32526 and No. DMR97-32763.

[1] G. A. Prinz, Phys. Today **48**, No. 4, 58 (1995).

[2] J. M. Daughton, A. V. Pohm, R. T. Fayfield, and C. H. Smith, J. Phys. D **32**, R169 (1999).

[3] R. A. de Groot, F. M. Mueller, P. G. van Engen, and K. H. J. Buschow, Phys. Rev. Lett. **50**, 2024 (1983).

[4] A. M. Bratkovsky, Phys. Rev. B **56**, 2344 (1997).

[5] K. Schwarz, J. Phys. F **16**, L211 (1986).

[6] S. P. Lewis, P. B. Allen, and T. Sasaki, Phys. Rev. B **55**, 10 253 (1997).

[7] N. E. Brener, J. M. Tyler, J. Callaway, D. Bagayoko, and G. L. Zhao, Phys. Rev. B **61**, 16 582 (2000).

[8] F. Y. Yang, C. L. Chien, E. F. Ferrari, X. W. Li, G. Xiao, and A. Gupta, Appl. Phys. Lett. **77**, 286 (2000).

[9] M. J. M. de Jong and C. W. J. Beenakker, Phys. Rev. Lett. **74**, 1657 (1995).

[10] S. K. Upadhyay, A. Palanisami, R. N. Louie, and R. A. Buhrman, Phys. Rev. Lett. **81**, 3247 (1998).

[11] R. J. Soulen, J. M. Byers, M. S. Osofsky, B. Nadgorny, T. Ambrose, S. F. Cheng, P. R. Broussard, C. T. Tanaka, J. Nowak, J. S. Moodera, A. Barry, and J. M. D. Coey, Science **282**, 85 (1998).

[12] The spin polarization measured with PCAR in the ballistic regime with negligible interface scattering is $P = (I^{\uparrow} - I^{\downarrow})/(I^{\uparrow} + I^{\downarrow})$, with spin-up ($\sigma = \uparrow$) and spin-down ($\sigma = \downarrow$) currents $I^{\sigma} \propto N^{\sigma} v_F^{\sigma}$. Here N^{σ} is the spin-dependent density of states at the Fermi level and v_F^{σ} the spin-dependent Fermi velocity.

[13] W. J. DeSisto, P. R. Broussard, T. F. Ambrose, B. E. Nadgorny, and M. S. Osofsky, Appl. Phys. Lett. **76**, 3789 (2000).

[14] G. J. Strijkers, Y. Ji, F. Y. Yang, C. L. Chien, and J. M. Byers, Phys. Rev. B **63**, 104510 (2001).

[15] G. E. Blonder, M. Tinkham, and T. M. Klapwijk, Phys. Rev. B **25**, 4515 (1982).

[16] X. W. Li, A. Gupta, T. R. McGuire, P. R. Duncombe, and G. Xiao, J. Appl. Phys. **85**, 5585 (1999).

[17] A. G. M. Jansen, A. P. van Gelder, and P. Wyder, J. Phys. C **13**, 6073 (1980).

[18] R. Meservey and P. M. Tedrow, Phys. Rep. **238**, 173 (1994).

[19] D. J. Monsma and S. S. P. Parkin, Appl. Phys. Lett. **77**, 720 (2000).

[20] D. J. Monsma and S. S. P. Parkin, Appl. Phys. Lett. **77**, 883 (2000).

[21] I. I. Mazin, A. A. Golubov, and B. Nadgorny, J. Appl. Phys. (to be published).

[22] J. S. Moodera and G. Mathon, J. Magn. Magn. Mater. **200**, 258 (1999).

[23] A. Gupta, X. W. Li, and G. Xiao, J. Appl. Phys. **87**, 6073 (2000).

[24] A. Gupta, X. W. Li, S. Guha, and G. Xiao, Appl. Phys. Lett. **75**, 2996 (1999).

[25] P. LeClair, H. J. M. Swagten, J. T. Kohlhepp, R. J. M. van de Veerdonk, and W. J. M. de Jonge, Phys. Rev. Lett. **84**, 2933 (2000).